Molecular Crystals and Liquid Crystals

ISSN: 1542-1406 (Print) 1563-5287 (Online) Journal homepage: http://www.tandfonline.com/loi/gmcl20

NMR Study of a Bimesogenic Liquid Crystal with Two Nematic Phases

E. E. Burnell, R. Y. Dong, A. Kohlmeier, M. G. Tamba, C. Welch & G. H. Mehl

To cite this article: E. E. Burnell, R. Y. Dong, A. Kohlmeier, M. G. Tamba, C. Welch & G. H. Mehl (2015) NMR Study of a Bimesogenic Liquid Crystal with Two Nematic Phases, Molecular Crystals and Liquid Crystals, 610:1, 100-107, DOI: 10.1080/15421406.2015.1025211

To link to this article: http://dx.doi.org/10.1080/15421406.2015.1025211

Published online: 06 Jul 2015.

Mol. Cryst. Liq. Cryst., Vol. 610: pp. 100–107, 2015

ISSN: 1542-1406 print/1563-5287 online
DOI: 10.1080/15421406.2015.1025211

NMR Study of a Bimesogenic Liquid Crystal with Two Nematic Phases

E. E. BURNELL,[1,*] R. Y. DONG,[2] A. KOHLMEIER,[3] M. G. TAMBA,[3] C. WELCH,[3] AND G. H. MEHL[3]

[1]Department of Chemistry, University of British Columbia, Vancouver, B.C., Canada
[2]Department of Physics and Astronomy, University of British Columbia, Vancouver, B.C., Canada
[3]Department of Chemistry, The University of Hull, Hull, United Kingdom

Recent interest in bimesogenic liquid crystals showing two nematic phases has led us to investigate the nematic mean-field interactions in these nematic phases by using rigid solutes as probes. The nematic potential that is modelled by two independent Maier-Saupe terms is successful in fitting the observed dipolar couplings (order parameters) of para-, meta- *and* ortho-*dichlorobenzene solutes in both the nematic phases of 39 wt% of 4-*n*-pentyl-4′-cyanobiphenyl (5CB) in α,ω-bis(4-4′-cyanobiphenyl)nonane (CB_C9_CB) to better than the 5% level. The derived liquid-crystal potential parameters* G_1 *and* G_2 *for each solute in the N and* N_{tb} *phases will be discussed. The most interesting observation is that* G_1 *(associated with size and shape interactions) is almost constant in the* N_{tb} *phase, whereas* G_2 *(associated with longer-range electrostatic interactions) has large variation, even changing sign.*

Thermotropic liquid crystals can exhibit a vast variety of phases, including nematic, smectic and cholesteric. Nematic phases have orientational order and smectic phases have in addition positional order, while cholesterics are essentially twisted nematic phases that consist of chiral molecules. It is also known that an underlying nematic phase (i.e. reentrant nematic) exists at temperatures below the smectic A phase [1]. This reentrant nematic phase is identical to the nematic phase that exists at temperatures above the smectic A phase. There has been much interest recently in compounds that exhibit two different nematic phases: a high-temperature normal nematic phase, N, and a lower temperature phase initially termed N_x [2] now called a nematic twist-bend phase, N_{tb} [2–6]. The precise nature and structure of this N_{tb} phase is a topic of current investigation.

NMR has proved to be a very powerful tool in the investigation of liquid crystals [7–11]. One very successful application involves the proton NMR of small, well characterized solutes which act as probes of the anisotropic environment [8, 12–15]. The NMR spectra are analyzed to give dipolar couplings between each pair of protons in the molecule, and

*Address correspondence to E. E. Burnell, Department of Chemistry, University of British Columbia, Vancouver, B.C., V6T 1Z1, Canada. E-mail: elliott.burnell@ubc.ca

Color versions of one or more of the figures in the article can be found online at www.tandfonline.com/gmcl.

these dipolar couplings are used to calculate molecular order parameters. These order parameters in turn provide information about the anisotropic intermolecular potential that causes the solute orientational order.

It has been demonstrated that in a collection of nematic liquid-crystal solvents, the orientational order of a number of essentially rigid solutes can be rationalized in terms of the presence of two independent anisotropic interactions [16] each of which can be described in terms of the classic Maier-Saupe, MS, mean-field potential [17, 18]. It is the varying importance of the two mechanisms in this MSMS treatment that leads to a liquid-crystal dependence of the molecular order tensor.

In this paper we review an NMR investigation of several small, "rigid" solutes in a liquid-crystal solvent that exhibits both N and N_{tb} phases [19] and we emphasize the information obtainable about the latter phase. The approach involves using the MSMS model [16] for the orientational ordering of the solutes.

We start by reviewing the MSMS model in which the anisotropic intermolecular mean potential is written

$$H_{Ls}(\Omega_s) = -\frac{3}{4}\sum_{i=1}^{2} G_{L,ZZ}(i)\sum_{\gamma}\sum_{\delta}\cos(\vartheta_{s,\gamma})\cos(\vartheta_{s,\delta})\beta_{s,\gamma\delta}(i) \tag{1}$$

where $\vartheta_{s,\gamma}$ is the angle the between the solute s molecular axis γ and the nematic director n. The term $i = 1$ is taken to represent short-range size and shape interactions and $i = 2$ longer-range electrostatic interactions. The $G_{L,ZZ}(i)$ are the liquid-crystal mean fields, and the $\beta_{s,\gamma\delta}(i)$ are some solute electronic property that interacts with the liquid-crystal field. For example, if $\beta_{s,\gamma\delta}(2)$ is the $\gamma\delta$ component of the molecular quadrupole, then $G_{L,ZZ}(2)$ is the mean electric field gradient felt by this quadrupole.

The order parameters that are readily calculated from this potential

$$S_{s,\gamma\delta} = \frac{\int d\Omega \left(\frac{3}{2}\cos\vartheta_{s,\gamma}\cos\vartheta_{s,\delta} - \frac{1}{2}\delta_{\gamma\delta}\right)\exp\left(-\frac{H_{Ls}(\Omega_s)}{k_BT}\right)}{\int d\Omega \exp\left(-\frac{H_{Ls}(\Omega_s)}{k_BT}\right)} \tag{2}$$

can be compared with experiment in order to test models for the anisotropic intermolecular potential. Experiments on a collection of different solutes in a variety of different nematic liquid-crystal solvents were fitted with liquid-crystal $G_{L,ZZ}(i)$ and solute $\beta_{s,\gamma\delta}(i)$ parameters [16]. Initially, fitting to a single MS potential term was attempted, with the result displayed in figure 1 (left side). The agreement between experiment and recalculated order parameters is a disaster. However, when two MS terms are used in the MSMS potential, the agreement between experimental and recalculated order parameters is now at the 5% level, Figure 1 (right side). This is excellent evidence that the MSMS model describes the anisotropic intermolecular potential in nematic phases quite well [16].

In general, only products $G_{L,ZZ}(i)\,\beta_{s,\gamma\delta}(i)$ can be determined from fitting to the experimental order parameters: if a specific mechanism is not employed, one of G or β must be specified – *i.e.* for a single MS mechanism there is one degree of freedom. Because $H_{Ls}(\Omega_s)$ contains the sum of two such $G\beta$ terms, there are 2^2 (or 4) degrees of freedom, and thus four parameters (G or β or a mix of G and β) need to be specified. As discussed in the original literature [16], we choose to define four $G_{L,ZZ}(i)$ parameters. The values of the β parameters then obtained by fitting to experimental order parameters depend on the choice of the four G parameters. The arbitrary choice of G parameters is: $G_{\mathrm{MM},ZZ}(1) = 1$, $G_{\mathrm{MM},ZZ}(2) = 0$, $G_{1132,ZZ}(2) = 1$ and $G_{1132,ZZ}(1) = G_{\mathrm{EBBA},ZZ}(1)$ where

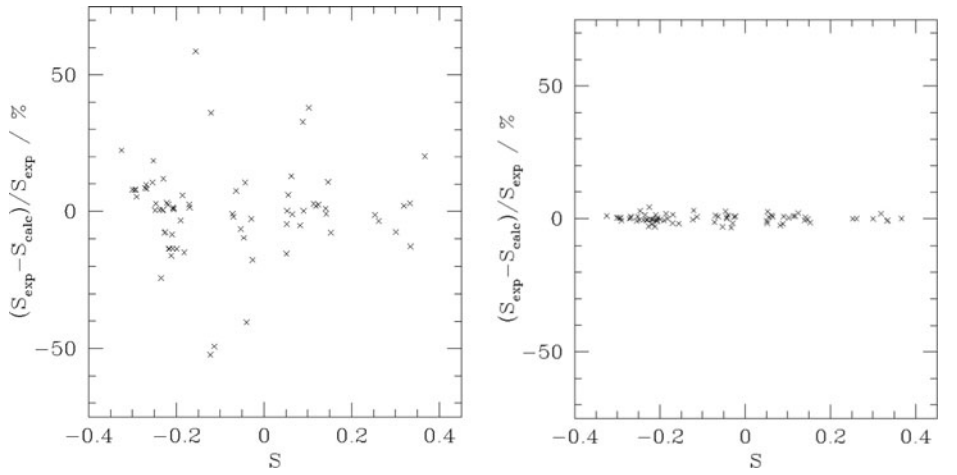

Figure 1. Left panel: percent difference between experimental and calculated order parameters *versus* *S*(experimental) using a single MS potential. Note that three of the points differ by over 100% and are not shown on the graph. Right panel: percent difference between experimental and calculated order parameters *versus* *S*(experimental) using two independent MS interactions, model MSMS. Reprinted with permission from [16].

MM is a magic mixture of the nematic liquid crystals Merck ZLI 1132 (1132) and *p*-ethoxybenzylidene-*p*′-*n*-butylaniline (EBBA). The orientational mechanism in MM is dominated by size and shape interactions only (which is why we set $G_{\mathrm{MM},ZZ}(2) = 0$) as indicated by experiments on di-deuterium which experiences zero electric field gradient in this mixture [15]. The G values for other nematic-phase solvents and all solute β parameters are based on these arbitrary definitions. The idea is that the solute $\beta_{s,\gamma\delta}(i)$ parameters are solute only properties which are independent of the liquid-crystal solvent, and hence values can be used for new nematic solvents: it is then only necessary to fit solute order parameters for a new solvent to obtain the new $G_{L,ZZ}(i)$ (hereafter written $G(i)$) values for the new solvent. Hence in this paper we use previously determined $\beta_{s,\gamma\delta}(i)$ values for dichlorobenzene solutes to "measure" the $G(1)$ and $G(2)$ values in the N and N_{tb} phases.

Mixtures of 4-*n*-pentyl-4′-cyanobiphenyl (5CB) in α,ω-bis(4-4′-cyanobiphenyl)nonane (CB_C9_CB) form the N_{tb} (labeled N_x in the figure) phase as shown in the phase diagram of Figure 2. Here we use a sample of 39 wt.% 5CB in CB_C9_CB in which the probe solutes 0.6 mol% *para*-dichlorobenzene (pdcb), 1.1 mol% *meta*-dichlorobenzene (mdcb) and 0.9 mol% *ortho*-dichlorobenzene (odcb) are dissolved. The N - N_{tb} phase transition was about 38°C. It is noted that the data corresponds to that reported in [20].

The proton NMR spectra of the solutes in the ordered N and N_{tb} phases of this sample are displayed in Figure 3. It is noteworthy that the lines in the spectra from the N_{tb} phase are much broader than those from the N phase. Dipolar couplings between all intramolecular proton pairs were readily obtained with spectral analysis using covariance matrix adaption evolutionary strategies (CMA-ES) [21–25]. The molecular order parameters were obtained using these dipolar couplings in conjunction with the published molecular structures of the solutes [26, 27].

The order parameters obtained by analyzing the dipolar couplings from the NMR spectra as a function of temperature in the N and N_{tb} phases are displayed in Figure 4, top

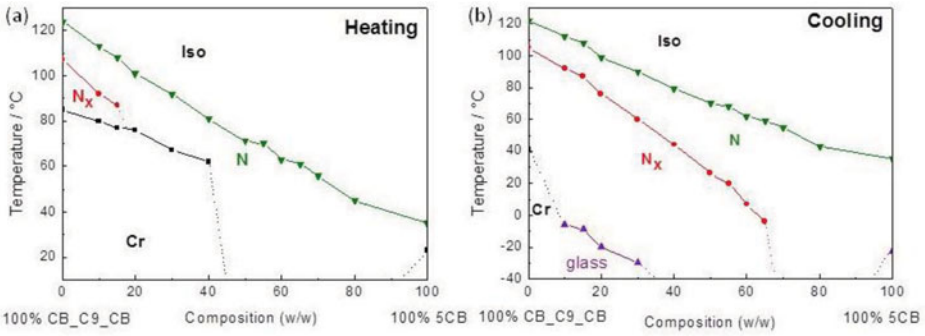

Figure 2. Phase diagram of the transition temperatures of the binary mixtures of dimer CB_C9_CB in 5CB, taken from the first DSC: (a) heating scans (10 $Kmin^{-1}$); (b) cooling scans (10 $Kmin^{-1}$).

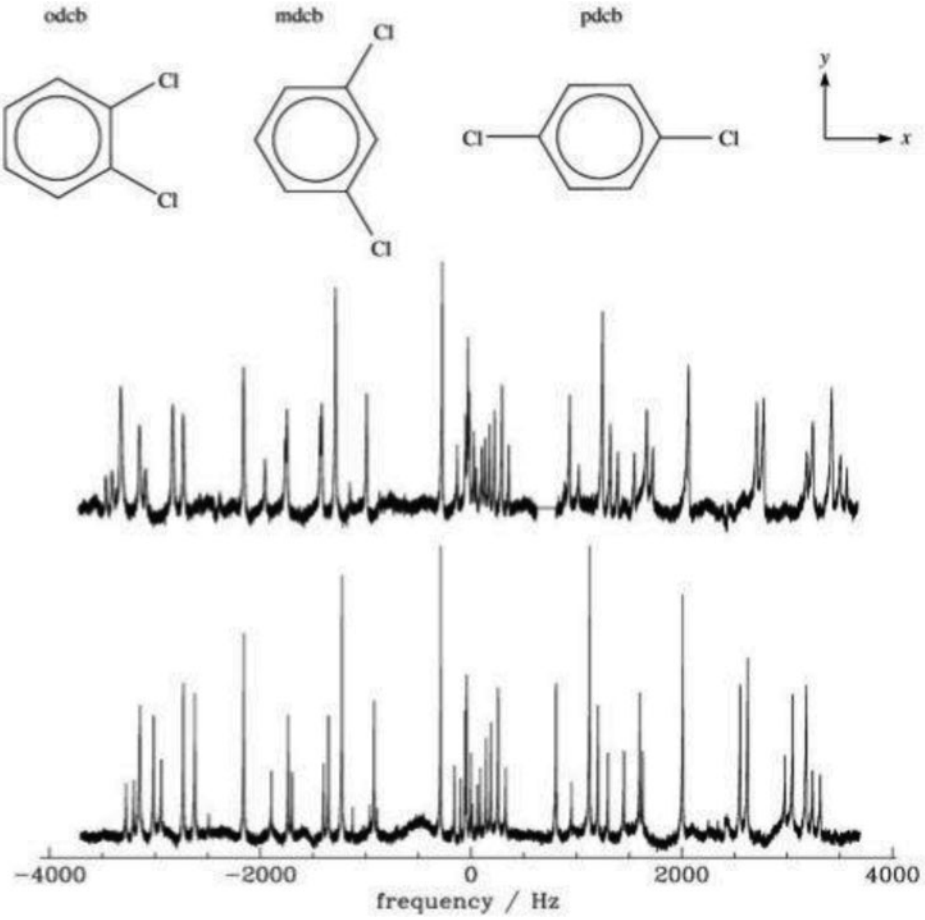

Figure 3. Molecular axis systems and proton NMR spectra of odcb, mdcb and pdcb dissolved in CB_C9_CB/5CB mixture (61/39 wt.%) at 34.5°C (top) in the N_{tb} phase and at 50°C (bottom) in the N phase. Reprinted with permission from [19].

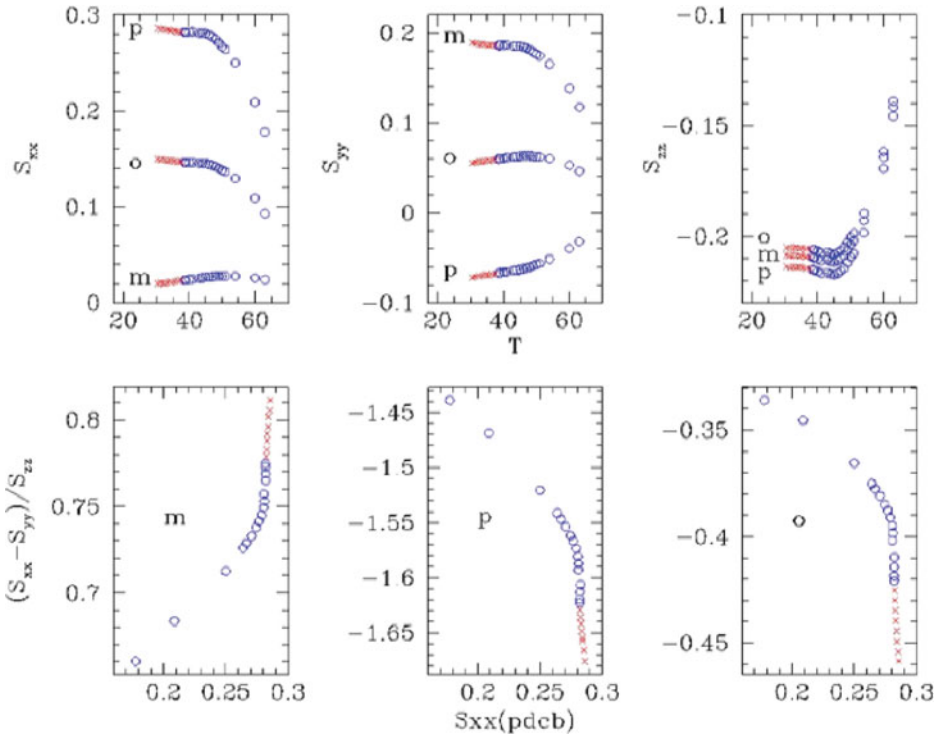

Figure 4. Order matrix elements for the three solutes odcb (o), mdcb (m) and pdcb (p) in the CB_C9_CB/5CB mixture in the N (open blue circles) and N_{tb} (red crosses) phases. The top three panels show S_{xx}, S_{yy} and S_{zz} as a function of temperature T. The bottom three panels show the order matrix asymmetry $(S_{xx} - S_{yy})/S_{zz}$ *versus* S_{xx}(pdcb) for the three solutes. The x axis is the molecular c_2 axis (for pdcb it is also the Cl–Cl axis), y is in the ring plane perpendicular to x, and z is perpendicular to the ring plane. Reprinted with permission from [19].

three panels. The N - N_{tb} phase transition for the liquid-crystal mixture used is at 38°C, and it can be seen in the figure that order parameters generally decrease in magnitude at higher temperatures in the N phase, then go through a pre-transitional region and become relatively constant in the N_{tb} phase. The asymmetry in the order tensor $(S_{xx}-S_{yy})/S_{zz}$ is plotted versus $S_{xx(pdcb)}$ in the lower panels, and for all solutes studied the pre-transitional behaviour in the N phase and the dramatic increase in absolute magnitude with decreasing temperature in the N_{tb} phase are clear. However, it is crucial to note that the order parameters are not completely constant in the N_{tb} phase. The deviations from constant are significant (the order parameters are obtained very precisely), and it is this deviation from constant that leads to the large variation in the asymmetry parameters and to the results for $G(1)$ and $G(2)$ obtained below.

The results obtained for the order parameters are interesting and unusual (normally, order parameters increase toward lower temperatures). To investigate these effects further, we use the MSMS model for solute orientational order and determine the liquid-crystal potential parameters $G(1)$ and $G(2)$ at each temperature. To do this we use the solute $\beta(i)$ parameters that were obtained for odcb, mdcb and pdcb in an earlier study [28]. The $G(1)$ and $G(2)$ values obtained are displayed in Figure 5. At higher temperature in the N phase, as

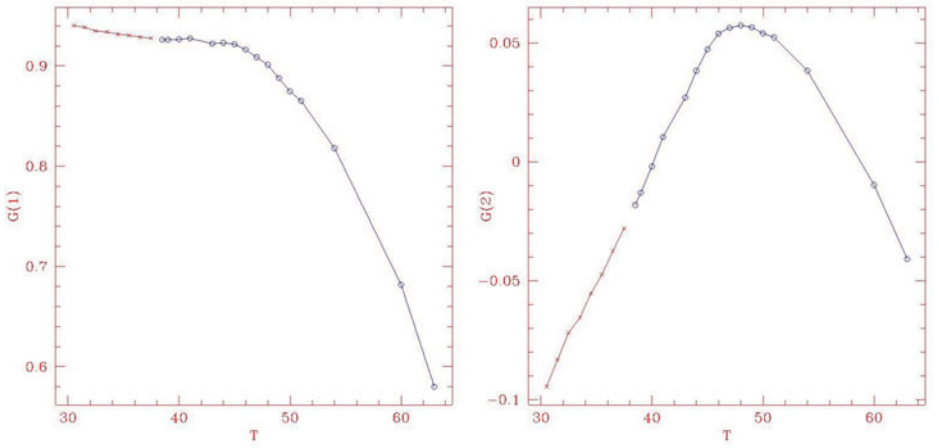

Figure 5. Nematic potential parameters $G(1)$ and $G(2)$ *versus* T for a global fit to order parameters of the three solutes odcb, mdcb and pdcb in the CB_C9_CB/5CB mixture that exhibits N (open blue circles) and N_{tb} (red crosses) phases.

expected and as observed experimentally for liquid-crystal phases generally, both $G(1)$ and $G(2)$ decrease with increasing temperature due to the lowering of the orientational order.

In the N_{tb} phase $G(1)$ is almost constant whereas $G(2)$ becomes more negative with decreasing temperature. Between these two limits, pre-transitional behaviour is noted in the N phase. The most interesting result is that in the N_{tb} phase only $G(2)$ changes significantly. There is good evidence to ascribe $G(1)$ to an orientational mechanism that depends on the solute size and shape, and $G(2)$ to longer-range electrostatic interactions, such as that between the solute polarizability anisotropy and the mean square electric field, or between the solute quadrupole and the mean electric field gradient that the solute feels in the anisotropic environment. Indeed, $G(2)$ is seen to change sign. If the interaction involved the solute quadrupole, the change in magnitude (and sign) of the interaction could possibly be explained in terms of the average local placement of the solute. In terms of interactions involving the quadrupole, this suggests that an alternative measurement of the liquid-crystal electric field gradient should be performed. Such an experiment is possible using molecular deuterium [15], and is planned. In this regard, D_2 is an excellent probe because its molecular properties are well documented. Analysis of the deuteron NMR spectrum yields both the deuteron quadrupole coupling B and the D—D dipolar coupling D_{DD}. The intramolecular contribution to both these couplings contains the molecular order parameter as a factor, and thus the ratio of the couplings should be a molecular constant. However, different experiments yield different ratios. This difference is a direct result of B having an extramolecular contribution due to the environment. The external mean electric field gradient felt by the deuteron nuclei is readily calculated from this extra contribution. It will be interesting to see whether the extra contribution mimics the $G(2)$ behaviour observed here.

The behaviour of $G(2)$ is dramatically emphasized in Figure 6 (left panel) in a plot of $G(1)$ versus $G(2)$. "Expected" behaviour ($G(1)$ and $G(2)$ both increase with decreasing T) is observed in the N phase at low $G(1)$ values (corresponding to higher T). Also the constant nature of $G(1)$ in the N_{tb} phase is clear, as is the pre-transitional behaviour. The decrease of $G(2)$ with decreasing T is dramatic in comparison to $G(1)$, and is a direct

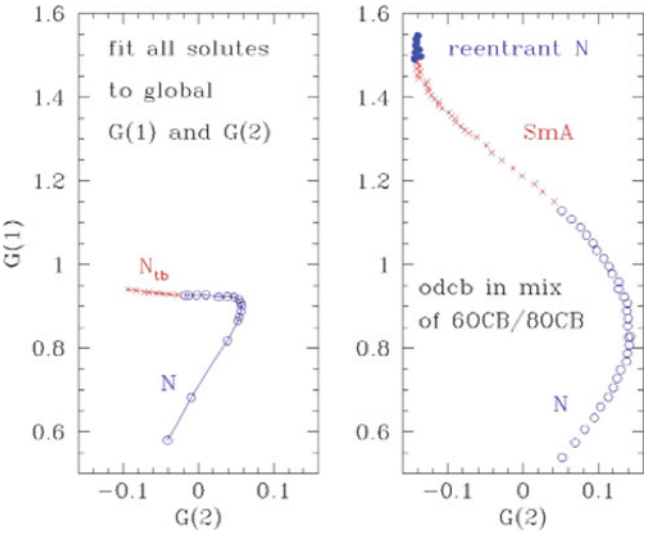

Figure 6. Nematic potential parameters $G(1)$ *versus* $G(2)$ for a global fit to order parameters of the three solutes odcb, mdcb and pdcb in the CB_C9_CB/5CB mixture that exhibits N (open blue circles) and N_{tb} (red crosses) phases (top) and of odcb in the 6OCB/8OCB mixture that exhibits N, SmA and RN (filled blue circles) phases (bottom). Reprinted with alterations with permission from [19].

consequence of the large change in asymmetry order parameter with T (see bottom panels of Figure 4). In the right panel, we compare the result for the N_{tb} phase with that of a different experiment involving a liquid-crystal mixture of 27 wt% 6OCB and 8OCB which forms a higher T nematic phase, a smectic A phase, and a lower T re-entrant-nematic phase. As in the present study for the N_{tb} phase, $G(2)$ is found to decrease with lower T in the smectic A phase. Of particular note is that $G(2)$ is found to increase slightly with lowering T in the re-entrant N phase, in agreement with the behaviour in the higher-temperature N phase. It is noted that freeze fracture TEM investigations of structurally closely related systems show periodicities in the range of 8–10 nm in the N_{tb} structure [29, 30]. More recent AFM data show the absence of features in the LC phase, indicating the ongoing need of investigating the structure of the N_{tb} phase with complimentary techniques [31].

In summary, our experiments demonstrate one dramatic property of the new N_{tb} phase, *i.e.* the results are consistent with the solute orientational ordering arising from two independent mechanisms. The first arises from solute size and shape effects, and is virtually constant in the N_{tb} phase. The second exhibits dramatic change in this phase, and arises from some longer-range electrostatic interaction. A likely candidate is the interaction between the solute quadrupole with the mean electric field gradient that the solute feels in the liquid-crystal solvent. We plan to check out this possibility with experiments using molecular deuterium.

Funding

MGT, CW and GHM acknowledge funding by the EU FP7 project BIND and the EPSRC through project EP/J004480/1. EEB and RYD acknowledge financial support from the Natural Sciences and Engineering Research Council of Canada.

References

[1] Cladis, P. E. (1975). *Phys. Rev. Lett.*, *35*, 48.
[2] Panov, V. P., *et al.* (2010). *Phys. Rev. Lett.*, *105*, 167801.
[3] Cestari, M., *et al.* (2011). *Phys. Rev. E*, *84*, 031704.
[4] Cestari, M., Frezza, E., Ferrarini, A., & Luckhurst, G. R. (2011). *J. Mater. Chem.*, *21*, 12303.
[5] Castles, F., Morris, S. M., Terentjev, E. M., & Coles, H. J. (2010). *Phys. Rev. Lett.*, *104*, 157801.
[6] Balachandran, R., Panov, V. P., Tamba, M. G., Mehl, G. H., Song, P. J. K., Panarin, Y. P., & Vij, J. K. (2014). *J. Materials Chemistry C*, *2*, 8179.
[7] *Nuclear Magnetic Resonance of Liquid Crystals*. Emsley, J. W., Ed. NATO Advanced Study Institute Series C 141, D. Reidel: Dordrecht, 1985.
[8] *NMR of Ordered Liquids*, edited by Burnell, E. E. & de Lange, C. A. (Kluwer Academic, Dordrecht, 2003).
[9] Dong, R. Y. *Nuclear Magnetic Resonance of Liquid Crystals*, 2nd ed.; Springer-Verlag: New York, 1997.
[10] *Nuclear Magnetic Resonance Spectroscopy of Liquid Crystals*; Dong, R. Y., Editor. World Scientific, Singapore, 2010.
[11] *MRC Special Issue on NMR of liquid crystals.* Dong, R. Y., Editor. (2014). *Magn. Reson. Chem. 52* (Issue 10).
[12] Buckingham, A. D. & McLauchlan, K. A. *Progress in Nuclear Magnetic Resonance Spectroscopy*; Pergamon Press: Oxford, 1967; Vol. 2, p 63.
[13] Diehl, P. & Khetrapal, C. L. *NMR Basic Principles and Progress*; Springer-Verlag: Berlin, 1969; Vol. 1, p 1.
[14] Emsley, J. W. & Lindon, J. C. *NMR Spectroscopy using Liquid Crystal Solvents*; Pergamon Press: Oxford, 1975.
[15] Burnell, E. E. & de Lange, C. A. (1998). *Chem. Rev. 98*, 2359 and references therein.
[16] Burnell, E. E., ter Beek, L. C., & Sun, Z. (2008). *J. Chem. Phys.*, *128*, 164901.
[17] Maier, W. & Saupe, A. Z. (1959). *Z. Naturforsch. A*, *14*, 882.
[18] Maier, W. & Saupe, A. Z. (1960). *Z. Naturforsch. A*, *15*, 287.
[19] Dong, R. Y., Kohlmeier, A., Tamba, M. G., Mehl, G. H., & Burnell, E. E. (2012). *Chem. Phys. Lett.*, *552*, 44.
[20] Tripathi, C. S. P., Losada-Perez, P., Leys, J., Kohlmeier, A., Tamba, M.-G., Mehl, G. H., & Glorieux, C. (2011). *Phys. Rev. E.*, *84*, 041707.
[21] Hageman, J. A., Wehrens, R., de Gelder, R., Meerts, W. L., & Buydens, L. M. C. (2000). *J. Chem.Phys.*, *113*, 7955.
[22] Meerts, W. L. & Schmitt, M. (2006). *Int. Rev. Phys. Chem.*, *25*, 353.
[23] Meerts, W. L., de Lange, C. A., Weber, A. C. J., & Burnell, E. E. (2009). *J. Chem. Phys.*, *130*, 044504.
[24] Weber, A. C. J., Yang, X., Dong, R. Y., Meerts, W. L., & Burnell, E. E. (2009). *Chem. Phys. Lett.*, *476*, 116.
[25] Burnell, E. E., de Lange, C. A., & Meerts, W. L. in *Nuclear Magnetic Resonance Spectroscopy of Liquid Crystals*, R. Y. Dong (Ed.), World Scientific Publishing Co., Singapore, 2010, p. 1.
[26] Syvitski, R. T. & Burnell, E. E. (1999). *Can. J. Chem.*, *77*, 1761.
[27] Syvitski, R. T. & Burnell, E. E. (2000). *J. Magn. Reson.*, *144*, 58.
[28] Weber, A. C. J., Yang, X., Dong, R. Y., & Burnell, E. E. (2010). *J. Chem. Phys.*, *132*, 034503.
[29] Borshch, V., Kim, Y.-K., Xiang, J., Gao, M., Jákli, A., Panov, V. P., Vij, J. K., Imrie, C. T., Tamba, M. G., Mehl, G. H., & Lavrentovich, O. D. (2013). *Nature Communications*, *4*, 2635.
[30] Gao, M., Kim, Y.-K., Zhang, C., Borshch, V., Zhou, S., Park, H.-S., Jákli, A., Lavrentovich, O. D., Tamba, M.-G., Kohlmeier, A., Mehl, G. H., Weissflog, W., Studer, D., Zuber, B., Gnägi, H., & Lin, F. (2014). *Microscopy Research and Technique*, *77*, 754.
[31] Gorecka, E., Salamonczyk, M., Zep, A., Pociecha, D., Welch C., Ahmed, Z., & Mehl, G. H. (2015). *Liq. Cryst.*, *41*, 1.